Design, fabrication and optical characterization of multi-component photonic crystals for integrated silicon microphotonics

Anna Baldycheva[a], Vladimir A. Tolmachev[b], Tatiana S. Perova[*a], Kevin Berwick[c], Yulia A. Zharova[b] and Ekaterina V. Astrova[b]

[a]Department of Electronic and Electrical Engineering, Trinity College Dublin, Dublin 2, Ireland;
[b]Ioffe Physical Technical Institute, Polytechnicheskaya 26, St. Petersburg, Russia;
[c]Department of Electronic and Communications Engineering, Dublin Institute of Technology, Kevin St, Dublin 8, Ireland

ABSTRACT

This paper reports on investigation and possible applications of the optical elements based on one-dimensional (1D) multi-component photonic crystal (PCs). The gap map approach and the transfer matrix method were used in order to mathematically describe multi-component 1D PC structures. We have found that the introduction of the additional regular layer into PC affects the properties of high-order PBGs, resulting in their vanishing in the certain range of the wavelengths and the formation of wide regions of total transparency instead. Tuning the number, position and width of these regions of total transparency in Si PCs has been demonstrated using the map of transmission bands. By analogy with multilayer dielectric coatings the additional component in multi-component Si PCs can be considered as an antireflection layer. The experimental results for the high-contrast multi-component PCs based on SiO_2-Si-SiO_2-Air structure with wide transmission bands are demonstrated in this study. The suggested approach can also be applied to the design of any micro- and nano- structured semiconductor or dielectric materials for application across wide electromagnetic spectrum.

Keywords: 1D Photonic Crystal, Tunable Photonic Crystal, Multi-component Photonic Crystal, Photonic Band Gap, Photonic Gap Map

1. INTRODUCTION

Miniaturization and integration of the optical devices, such as filters, polarisers, splitters and switches in electro-optical microcircuits is the key goals for realisation of all Si based microphotonics [1]. One of the great expectations is associated with the research and development of the optical devices operating on photonic band gap (PBG) effect, namely devices based on Si Photonic Crystal (PC) structures [2,3]. Owning to the PBG effect, which is the total reflection of all frequencies of light within this gap; Si PCs are used as broadband Bragg mirrors or reflectors [4]. The operational wavelength of these devices possesses a high sensitivity to the refractive indices, n, and thickness, d, of all the components of PC. The Si-based PCs are normally composed of two-components, which are primarily Si with high refractive index $n_H = n_{Si}$ and any other material with lower refractive index $n_L < n_{Si}$. Furthermore, by changing the value of n_L, tuning and switching ON- and OFF- of the PBGs can be achieved [5]. By variation of the refractive index of one of the PC component, using the external forces, or by introducing any disorder of the components in PC structure the narrow transmission peaks can be formed within the PBG. Thanks to these narrow transmission peaks a variety of Si PC band-pass filters have been proposed nowadays [6-9]. By varying the angle of incidence of light these Si PC band-pass filters, which reflect or transmit the certain polarization, can be designed[10].

*perovat@tcd.ie; phone 3 531 896-1432; fax 3 531 677-2442; http://www.mee.tcd.ie

Silicon Photonics VI, edited by Joel A. Kubby, Graham T. Reed, Proc. of SPIE Vol. 7943,
79430F · © 2011 SPIE · CCC code: 0277-786X/11/$18 · doi: 10.1117/12.875656

Recently, a new model of multi-component PCs has attracted a great attention of researchers [11-14]. The effect of tuning and switching of PBGs in multi-component PCs can be achieved by variation of the optical thickness of the additional regular components. For Si-based PCs it was shown that variation of the thicknesses of the additional component, for example SiO_2 or Si_3N_4, can be performed with the high accuracy, thus providing one with the precise engineering of the optical properties in PBG devices[14]. In other words the multi-component PC with the additional component of certain thickness can be an equivalent to the ordinary two-component Si PC infiltrated with the certain filler. At the same time, from the practical point of view, precise alteration of the thicknesses of the additional components can be easier and more effective than changing and finding of the fillers in ordinary PC device.

In this paper, we have focused on the investigation of 1D multi-component PCs based on grooved Si with an additional regular component. The 1D structure was chosen due to certain advantages over the other type of PCs that mainly related to their simpler fabrication and integration into photonic integrated circuit and the possibility of formation the omni-directional bands (ODBs) [15-17] at the same time. Using the Gap Map (GM) approach[18] we have demonstrated that the introduction of the additional SiO_2 component into 1D PC mirror can, under certain conditions, result in the disappearance of certain number of the PBGs in the extended range of Si filling factor. We applied the GM approach to generate the map of transmission bands (TBs) in order to observe the effect in the entire range of Si filling factor and in a wide wavelength range. The generated maps of TBs have demonstrated the formation of the ultra-wide transmission bands over the suppressed PBGs in a whole range of possible filling factors. The obtained TBs exhibit a high transmission value (T> 0.99) and a substantial bandwidth for the oblique incidence of light. These wide regions of transparency can be utilized for fabrication of antireflective structures for integrated photonic devices, optical biochemical sensors, as well as tunable polarizers operating in a wide range of angles of incidence. Based on the generated map of TBs the PC filter with ultra-wide pass-band characteristics have been successfully fabricated and characterized.

2. DESIGN CONSIDERATIONS AND THEORETICAL CALCULATIONS

2.1 Modeling of multi-component photonic crystal structure

Micro-structured Si with deep linear grooves [19] is considered here as a model for the ordinary 1D PC structure. This structure consists of alternating layers of materials with high, n_H, and low, n_L, refractive indices. The refractive index of Si for the H-component in the IR range is chosen to be $n_{Si}=n_H=3.42$. The refractive index of air for the L-component is $n_{air}=n_L=1$. In this case, the refractive index contrast is $\Delta n=n_H/n_L=3.42/1$ and the obtained PC can be considered as a high-optical contrast PC. Therefore, only a small number of periods, m, is required to obtain a PBG with a reflection of greater than 0.99. Let us consider an example of this 1D PC with the number of periods m=5. The refractive index of the incoming and outgoing medium, n, is taken as 1. We would like to investigate the impact on optical properties caused by insertion of an additional regular t-layer with a refractive index $n_t < n_{Si}$ (for example $n_t = 1.5$), which can be deposited or grown on the Si walls of the 1D PC structure with a definite lattice constant, $A=D_H+D_L$, where D_H and D_L are thicknesses of H and L- components, respectively (Fig. 1).

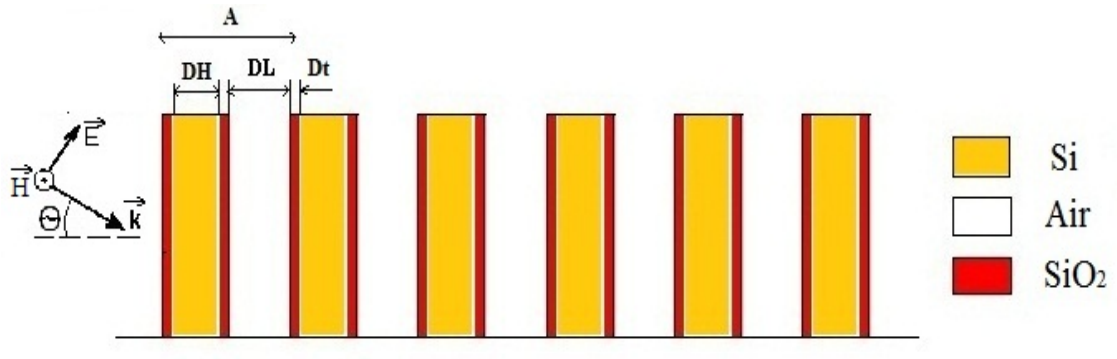

Fig. 1. Schematic fragment of multi-component 1D PC for the model with fixed value of the lattice constant A. The thicknesses of H, L and t layers are D_H, D_L, D_t, accordingly.

Calculations of the reflection and transmission spectra of 1D PCs with a filling factor of the Si walls $f_{Si}=D_H/A$, are performed using the Transfer-Matrix Method (TMM) [20]. This method is attractive due to the ease of introduction of an arbitrary number of additional layers at any point in the TMM's equation. As demonstrated earlier the best analysis of the optical properties of PC structures can be performed using a combination of simulated by TMM reflection/ transmission spectra and GM approach[21-25]. In the course of the GM calculations we assume that the lattice constant A and the t-layer thickness, D_t, do not change, since the t-layers with refractive index n_t were introduced on both sides of the Si wall (H-component) in our PC structure. To create a GM of PBGs or stop-bands (SBs) we need to generate the set of reflection spectra for each value of the filling factor $f_{Si}=D_H/A$ ranging from 0 to 1. Next, values of frequency satisfying the required criterion for PBG formation (R>0.99) are selected. However, when drawing the GM for a multi-component PC, the range of possible Si filling factors $f_{Si}=D_H/A$, required for the formation of SBs, is reduced to below a specific value of $maxf_{Si}=(A-2D_t)/A$ [14,26]. The limit, placed on the value of f_{Si}, is due to the fact that the value of D_L decreases as a result of the introduction of the additional components. When generating f_{Si}, the values of D_H for both two-component and the three-component PCs are the same and, therefore, we can compare two different PC structures using a single f_{Si} scale.

Utilization of the GM approach gives a visual representation of the transformation of the PBG areas during the transition from a two-component to a multi-component PC[14, 26]. The GM approach enables us to choose the parameters required for the engineering of the optical devices based on grooved Si [19], which have application in integrated microphotonics. In particular, we can identify the range of frequencies that can be practically realized for these structures, and, therefore, establish the design criteria for different regions of the infra-red (IR) spectrum. All the optical characteristics, presented in this study, utilize the normalized frequency $NF=A/\lambda$ units and, therefore, can be applied to a wide range of structure sizes, including micro- and nano-structures.

2.2 Suppression of Stop Bands in 1D Bragg Mirror

In Figure 2 we compare the GMs over a wide range of NF for an ordinary two-component "*Si-Air*" PC (grooved Si) and for multi-component PC based on the same "*Si-Air*" structure after introduction of the regular t-layer with thickness of D_t= 0.10A. It is apparent that the lower SBs are least affected by the addition of the t-layer, retaining a similar area and experiencing a negligible red shift in frequency. At the same time, inspection of the high-order SBs over the entire range of NF, reveals regions of frequency, or equivalently wavelength, for which SBs are suppressed, with R<0.99. Note that the SBs determined for the original "*Si-Air*" PC structure are not suppressed over the entire NF range (Fig.2). A detailed examination of the suppressed high-order PBGs in these frequency regions reveals that SBs are not only

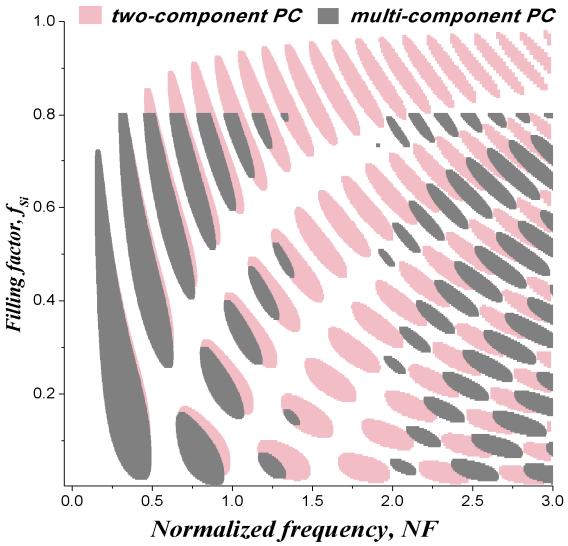

Fig. 2. GMs for a two-component *Si-Air* PC (light regions) and for a multi-component PC with n_t=1.5 and D_t=0.10A (dark regions) over a wide range of NF; $maxf_{Si}$=0.80. The calculations are performed at normal incidence of light with number of periods m=5.

significantly suppressed, but can actually disappear, with R=0. It is obvious that the regions of transmission could appear in these regions of frequency instead. Let us calculate a set of transmission spectra for a multi-component 1D PC with a t-layer thickness of D_t=0.1A over a range of f_{si} values from 0.08 to 0.1 with a step size of δf_{Si}=0.001 (Fig. 3(a)). Indeed, the transmission bands (TBs) are formed between the suppressed PBGs, with R less than 0.99. It is clear from Fig. 3(a) that the TB's range is constant for filling factors, f_{Si}, in the range 0.083 to 0.093, that is, with a change in the filling factor of Δf =0.093-0.083=0.01. Additional detail can be seen in Fig. 3 (b), where the transmission range is expanded across the range of transmissions from 0.97 to 1 in order to increase the clarity of the diagram. As shown in Fig. 3(b), the width of the TBs is also dependent on the selection of the cutoff transmission value. For example, if a cutoff transmission was chosen as 0.995, then the TBs within a narrow range of NF will appear narrower and less uniform than those for a cutoff level of 0.99. The choice of an appropriate cutoff level is an important design criterion when engineering practical device structures. Let us consider an example of the design of a real band-pass filter based on the three-component PC model from Fig. 3. Suppose the lattice period, A, is 3000 nm and the Si-wall thickness, D_H= f_{Si}·A, is 260 nm, corresponding to a filling factor f_{Si}=0.087. According to Fig. 3b, such an optical filter has a wide pass-band with bandwidth of 0.36 NF (350 nm) centered at NF=1.7 or a wavelength λ=A/NF=1760 nm. From Fig. 3a the filling factor deviation Δf_{Si} is up to 0.03, which corresponds to the possible Si wall thickness deviation ΔD_H=30 nm for this particular example filter.

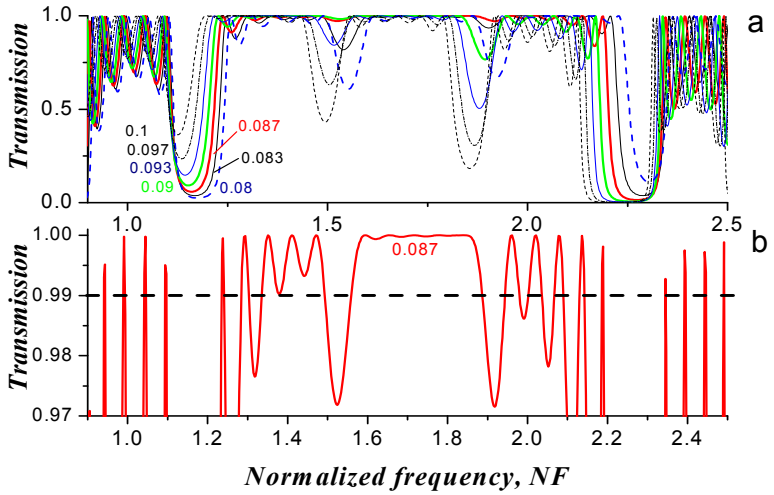

Fig. 3. The transmission spectra T for multi-component PC with t-layer refractive index n_t=1.5 and thickness D_t=0.10A for (a) f_{si}=0.08…0.1. (b) The same as in figure (a) shown for clarity in expanded transmission scale for f_{si}= 0.087. The calculations are performed at normal incidence of light with number of periods m=5.

2.3 Influence of the additional component thickness on the formation of transmission bands.

Now that we have established the general criteria for TB formation, we can plot a map of the regions of transparency (RTs) for the multi-component PC by analogy with the GM for PBGs[10, 21]. In order to avoid plotting very narrow peaks with high transmission, T>0.99, from the spectrum in Fig. 3(b) (see, for example, peaks at NF=1, 2.2, 2.4) we need to define a minimum range of ΔNF>0.01, which provides transmission values T>0.99. Removal of the narrow regions, by defining ΔNF<0.01 greatly improves the clarity of the TBs. In Figure 4 (a) the map of TBs is demonstrated with the GM, simulated for the "Si-Air" PC structure with additional component with refractive index n_t=1.5 and thickness D_t=0.13A. It is apparent, that the TB regions are located between the SBs areas of the corresponding PC structure. Note the total suppression of high order SBs over a range of NF from ~1.1 to ~1.5. This NF range also contains the widest TBs. This is also confirmed by the transmission spectrum, shown below in Fig. 4 b. Therefore, we conclude that the third layer in 1D PC structure can be treated as an antireflection layer by analogy with multilayer dielectric coatings.

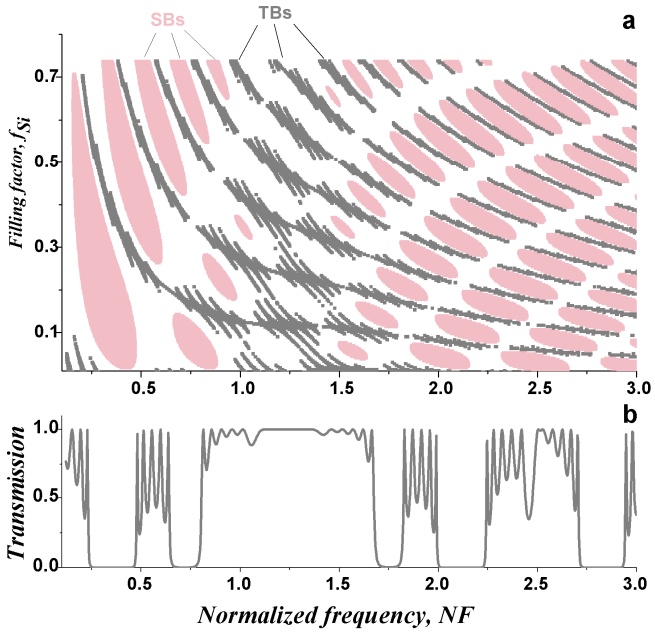

Fig. 4. a) The GM of stop-bands (R>0.99), denoted as *SBs*, and map of transmission bands (T>0.99), denoted as *TBs*, for the multi-component PC with n_t=1.5and D_t=0.13A. b) The transmission spectrum T for the same multi-component PC for f_{si}=0.117. The calculation is performed at normal incidence of light with number of periods m=5.

It should be noted that the SBs determined for the ordinary PC structure, shown in Fig.2, are not suppressed over the whole *NF* range and, therefore, originally have no wide TBs in this range.

Let us now analyze the changes that occur in these wide TBs, when the thickness of the additional t-layer is varied, using maps of the transparency regions. For this purpose, maps of TBs for the three-component PC with t-layer thicknesses D_t=0.20A and D_t=0.33A were calculated (Fig.5). The calculation procedure, used to determine the TBs, and the form of their graphical representation are the same as that described earlier.

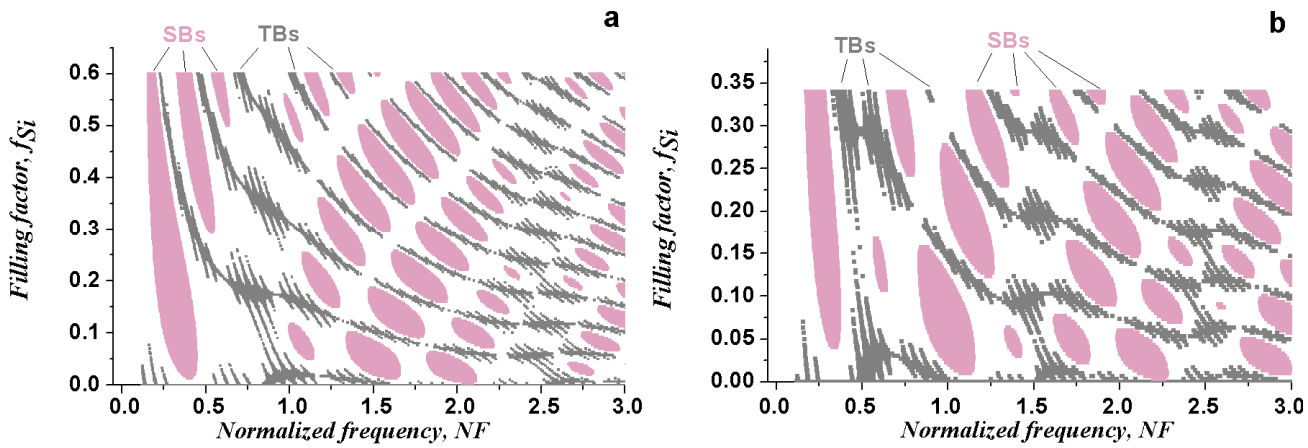

Fig. 5. a) The GMs of PBGs (denoted as *SBs*) and maps of TBs (denoted as *TBs*) for the multi-component PC with additional t-layer of refractive index of n_t=1.5 and thicknesses (a) D_t=0.20A and (b) D_t=0.33A. The calculation is performed at normal incidence of light with number of periods m=5.

It is worth noting that, for the PC with D_t=0.20A, the TBs exhibit a different behavior than for the case of D_t=0.13A. The widest TBs disappear between 1.1 and 1.4, reappearing again in two *NF* regions, viz. from 0.5 to 1.1 and from 2.3 to 2.6. As shown before, these features were not observed for the ordinary two-component PC with optical contrast 3.42/1 (see Fig. 2 a, light grey curves). Moreover, as expected, for an additional layer thickness of D_t=0.33A, we can already see the

formation of three regions with wide TBs over the same *NF* range. Thus, an increase in the *t*-layer thickness results in an increase in the number of TBs. Therefore, by changing the thickness values of *t*-layer we can manipulate with width and number of TBs in Si PC device.

2.4 Influence of the oblique incidence of light on regions of transparency

Based on the preliminary calculations performed in section 2.3, we have successfully demonstrated how the thickness of the *t*-layer is affecting the formation of the regions of transparency in multi-component Si photonic crystal. The next important issue, which needs further investigation, is the impact of oblique incidence of light on TBs. As it was demonstrated earlier [18, 25], the PBGs cannot be obtained at certain angles of incidence of light for 1D "*Si-Air*" PC structures, regardless of the filling factor f_{Si}. In the paper [14] we have shown, that by lowering the effective optical contrast (e.g. from high to medium) due to introduction of the additional components, one can obtain the omni-directional SBs in initially high-contrast structures. The calculated omni-directional SBs for multi-component PC structure have even larger width, than those for the equivalent two-component structures with medium optical contrasts, for both TM and TE polarizations of light. The TM and TE are the Transverse Magnetic and Transverse Electric polarizations of electromagnetic wave, respectively.

Let us consider now the multi-component "*Si-Air*" PC system with the additional *t*-layer of the thickness D_t=0.2*A*. A detailed analysis have shown that an increase of the angle of incidence of light, θ, does not affect significantly the formation of TBs, which are experiencing only a blue shift in an entire range of f_{Si}. At the same time, a large increase of the angle of incidence (θ >50º) leads to the widening of TBs for TM polarization and their narrowing for TE polarization. On the contrary, as was demonstrated in the past, the width of the SBs for TE polarization increases with an increase in θ, while for TM polarization it decreases [10]. Therefore, we can expect that at certain conditions the wide SBs for TE polarization may overlap with the wide TBs for TM polarization. The

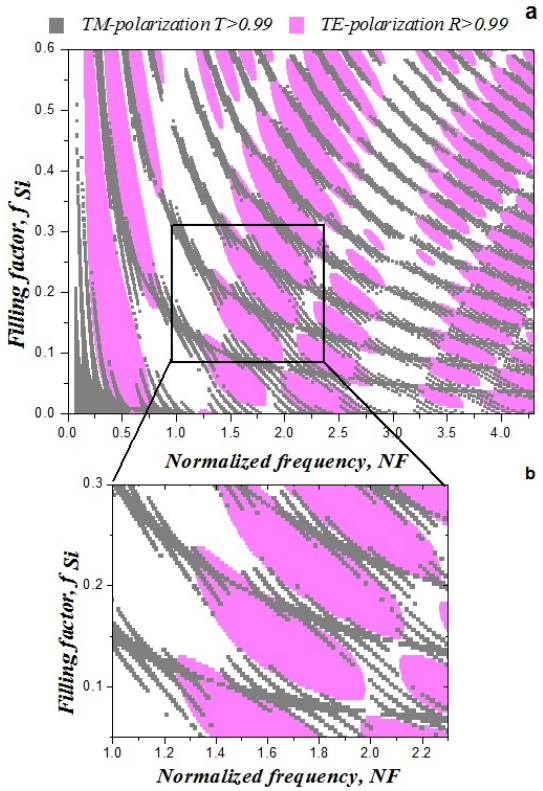

Fig. 6. The GM of SBs (*R*>0.99) for TE-polarization (light regions) and map of TBs (*T*>0.99) for TM-polarization (dark regions) for the multi-component PC with D_t=0.2*A* in a wide f_{Si} range (a) and in limited f_{Si} range (b). The calculation is performed at angle of incidence θ= 60°.

overlapping regions determine the regions of frequency for which a multi-component PC structure is totally transmitting the TM-polarized light and totally reflecting the TE-polarized light, and, therefore, this structure is acting as a highly efficient polarizer. In Figure 6a, we demonstrate the GM, calculated for θ=60^o for TE-polarization, which is compared to the map of TBs, calculated for the same angle θ but for TM-polarization of the incident light. It is apparent from Fig.6a that the TBs have partially overlapped with SBs in a whole range of f_{Si}. For clarity, the same maps are demonstrated in the limiting range of f_{Si} and *NF* in Figure 6b. It is clearly seen, that the overlapped regions can reach the width up to 0.05 *NF* for certain values of f_{Si}. For the example considered here, A=3 μm, this width value is equaivalent to approximately 60 nm. In order to demonstrate the overlapped regions in details, as well as to show the qualities of the obtained TBs in transmission spectra, the *T*-spectra for both polarizations were calculated using a filling factor f_{Si}=0.18 (Fig.7). The overlapped regions for both polarizations correspond to the maximum value of *T* for TM polarizion and the minimum value of *T* for TE polarization. It is also apparent, that the overlapped regions (with T>99%) demonstrate a negligible number of ripples on the top.

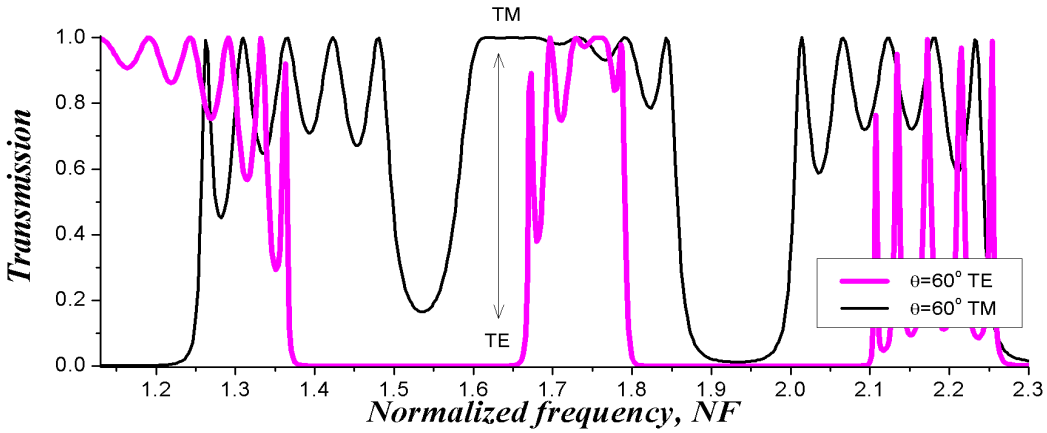

Fig. 7. The *T* spectra for f_{Si}=*0.18* calculated for the multi-component PC with D_l=0.2A at angle of incidence θ= 60^o. The formation of TB for TM-polarization and SB for TE-polarization at *NF*= 1.62 demonstrates the transformation of the PC into TM-polarizer in transmission mode and TE-polarizer in reflection mode.

We conclude that the introduction of the additional, regular layer into a high optical contrast 1D PC, like for example grooved Si, results in the appearance of wide regions of transparency for TM polarization for an oblique incidence of light. Using an appropriate design a photonic crystal polarizer, based on grooved Si, can be fabricated for efficient operation with *T*>99% for TM polarization and *R*>99% for TE polarization in a specific wavelength regions over a wide range of the incident angles of light.

3. FABRICATION OF MULTI-COMPONENT 1D PHOTONIC CRYSTAL- AN EXAMPLE OF BAND-PASS FILTER.

Let us use the suggested in the previous section maps of TBs for the fabrication of the real band-pass optical filter with wide bandwidth operating in a mid-infrared (MIR) wavelength range. In order to introduce the third component into original two-component structure, we exploited thermal oxidation of the grooved Si structures. While other complex and more expensive deposition techniques, such as chemical vapour deposition or sputtering, can be used to deposit dielectric layers, thermal oxidation of Si has the advantage of having a better growth isotropy, especially for narrow, deep trenches and precise control of the grown thickness. Also the fundamental limitations of fabricated Si based devices, such as high roughness and corrugation of the etched Si surfaces, can be overcomed by oxidation smoothing. In the course of the model calculations we have to pay attention to the following important issues. Firstly, owing to the strong absorption band of $Si0_2$ around 9 μm in MIR range of spectra, the imaginary part of $Si0_2$ refractive index, n_{SiO2}, has been taken into account[27]. As will be demonstrated later this fact does not affect significantly the TBs or pass-bands (PBs) properties of the proposed filter. Secondly, during thermal oxidation the 44% of oxide thickness is formed at the expense of Si wall while the remaining 56% of the oxide grows outside in the air. Therefore, the maximum f_{Si} of resulting three-component

device will be reduced by the value $\Delta f_{Si} = (2 \cdot 0.44 \cdot D_{SiO2})/A$. For fabrication convenience let us use the original grooved Si structure with a lattice period A= 4 μm and the thickness of the additional component D_{SiO2}=0.18A. Only three silicon-air paired layers with m=3 are needed in order to demonstrate the SBs formation and their further replacement with TBs, making the device extremely compact and potentially low loss.

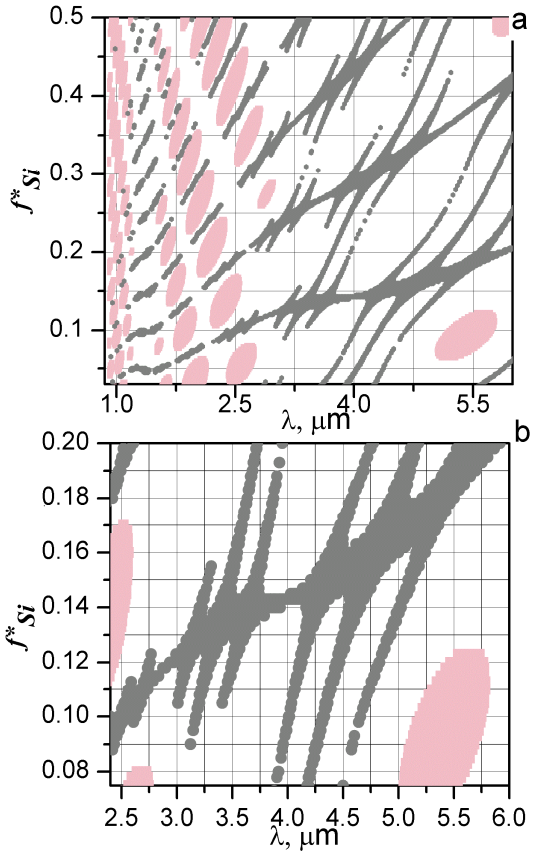

Fig. 8. (a) The GM of SBs with R>0.99 (light regions) and map of TBs with T>0.99 (dark regions) calculated for fabricated filter based on PC structure SiO_2-Si-SiO_2-Air with m=3 for mid-IR. (b) The same maps, demonstrated in the limited range of λ and f^*_{Si} for clarity. The dispersion of SiO_2 in MIR range and normal incidence of light θ=0 are taken into account during calculations.

Figure 8a shows the maps for the discussed structure calculated in a wide range of $f^*_{Si} = f_{Si} - \Delta f_{Si}$ from near-infrared to mid-IR spectral ranges. As can be seen for this figure, the introduction of the regular SiO_2 layers in the device (Fig.1) has affected the formation of SBs significantly. The limited number of high-order SBs have been vanished in a full range of f^*_{Si} over two wavelength regions (around 4 μm and 1.5μm). At the same time the regions of high transparency with T>99 % (dark regions) have become significantly wider in the same wavelength regions. It is also clear that the widest TBs are observed for the filling factor values less than 0.5, which actually corresponds to more realistic structures. According to TB's map the final device should have a filling factor f^*_{Si}=0.145 and, therefore, the final Si-wall thickness, $D_H = f^*_{Si} \cdot A$=0.58 μm. In the Fig. 8b the same map is presented in the limited range of f^*_{Si} from 0.075 to 0.2 in order to study the TBs and SBs for the proposed structure in details. It is obvious that the filling factor deviation, which corresponds to the pass-bands of the same bandwidth and centered at the same wavelength λc, is up to 0.015. Thus, the fabrication tolerance can be easily estimated from the proposed TB's map, which constitutes 60 nm for the particular demonstrated example filter.

For the fabrication of the original grooved structure we used a fabrication process that was described in details by Tolmachev [19]. The anisotropic chemical etching of (110) Si by KOH was used for the initial step. The depth of etching was 15 μm. Following this, grooved structure was thermally oxidized at the temperature T=900 °C for 120 min in order to grow an oxide layer of the thickness D_{SiO2}= 0.18A=720 nm on the top of Si side-walls. Thickness control of the SiO_2 layers was performed on witness samples using Spectroscopic Ellipsometry (see Ref. [28] for details). The R and T

spectra measurements have been performed using an FTS 6000 FTIR spectrometer in conjunction with a UMA IR microscope[29]. The aperture of the focused IR beam was 15 × 15 μm^2 and the spectral resolution was 8 cm^{-1}. A golden mirror was used as a 100% reference for measurements of reflection spectra. All measurements have been performed for normal incidence of light.

Figure 9 shows the experimental *R* and *T* spectra in comparison with the simulated ones. Apart from some excess losses, which may be due to optical scattering, there is good agreement between experiment and calculation. We note that the original grooved Si structure has the SBs centred at 3.5 μm and 4.8 μm. Thus, the original device is acting as a stop-band filter (Fig. 9a), while after thermal oxidation these SBs have been replaced with ultra-wide TB with bandwidth of 1400 nm in the range of wavelength from 3.4 μm to 4.8 μm. The obtained device can now operate as band-pass filter (Fig 9b). The utilization of the thermally grown SiO_2 for the fabrication of the multi-component PC device has resulted in the appearance of the negligible number of ripples (with depth up to 4-5%) on the otherwise flat-top transmission. Therefore, the fabricated band-pass filter can provide an ultra-wide transmission of 95-96% centred at 4.2 μm.

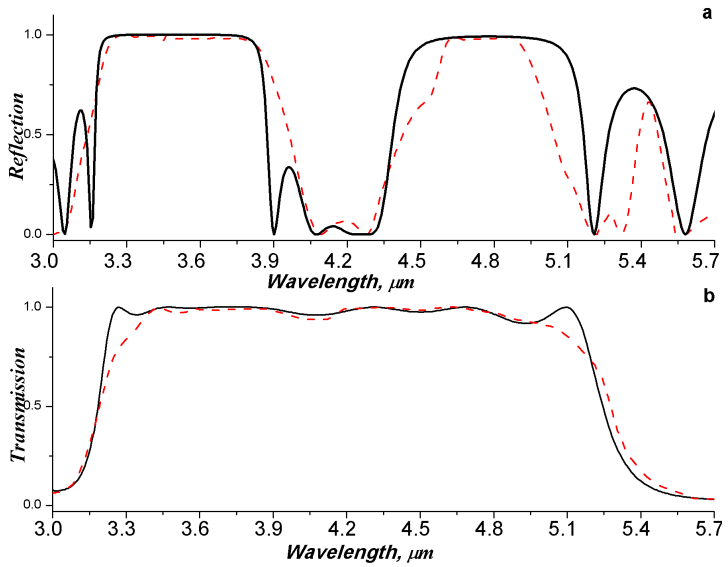

Fig. 9 (a) Experimental (dashed line) and calculated (solid line) *R* spectra of the band-stop filter based on two-component PC structure *Si-Air* with m=3 before thermal oxidation; filling factor f_{Si}=0.3. (b) Experimental (dashed line) and calculated (solid line) *T* spectra of the band-pass filter based on the same PC structure SiO_2-Si-SiO_2-Air after thermal oxidation; filling factor f^*_{Si}=0.145. The spectra demonstrate the transformation of the SBs at 3.5 μm and at 4.8μm into the TB at the wavelength λ_c= 4.2 μm.

This compact Si-based band- pass filter with ultra-wide and flat-top transmission characteristics may find a number of applications, such as antireflective structures, polarizers or optical sensors for biochemical molecules integrated into photonic and electro-optical devices.

CONCLUSION

The multi-component PC has been investigated by modeling them as two-component PC (grooved Si) with an additional regular component. The advantage of the multi-component Si PC structures for possible application in photonic integrated circuits has been demonstrated using the effect of disappearance of certain number of stop-bands and their replacement with wide pass-bands (T>99%). The Gap Map approach has been successfully demonstrated as the universal tool for designing of the optical components based on multi-component PCs structures. Using this approach enables full visualization of the obtained SBs and wide TBs in the entire range of the filling factors. By varying the thickness of the additional layer, the number and the width of the TBs can be changed. With increase of the angle of incidence the wide TBs for TM-polarization may partially overlap with SBs for TE-polarization, transforming the multi-component PCs into TM-polarizer in transmission mode and TE-polarizer in reflection mode. High-contrast, multi-component SiO_2-Si-SiO_2-Air PC based on grooved Si with thermally grown oxide layer SiO_2 has been fabricated and characterized. The obtained experimental results demonstrate a good agreement with the theoretical simulations.

Acknowledgments

This work has been supported by the ICGEE Programme (funded by IRCSET, Ireland), the Russian Foundation for Basic Research (project no.09-02-00782) and grant for support of leading scientific schools (NSh-3306-2010.2).

REFERENCES

[1] Soref, R. A., [Silicon-Based Microphotonics: from Basics to Applications], Amsterdam, 1-17 (1999).
[2] Yablonovitch, E., "Inhibited Spontaneous Emission in Solid-State Physics and Electronics," Phys. Rev. Lett. 58(20), 2059-2062 (1987).
[3] John, S., "Strong localization of photons in certain disordered dielectric superlattices," Phys.Rev.Lett., 58(23), 2486-2489 (1987).
[4] Lorenzo, E., Oton, C. J., Capuj, N. E., Ghulinyan, M., Navarro-Urrios, D., Gaburro, Z. and Pavesi, L., "Porous silicon-based rugate filters," Appl. Opt. 44(26), 5415-5421 (2005).
[5] Busch, K., Lölkes, S., Wehrspohn, R., Föll, H., [Photonic Crystals. Advances in Design, Fabrication, and Characterization], Weinheim: Wiley-VCH (2004).
[6] Yun, S.-S. and Lee, J.-H., "A micromachined in-plane tunable optical filter using the thermo-optic effect of crystalline silicon," J. Micromech. Microeng. 13, 721–725 (2003).
[7] Yi, Y., Bermel, P., Wada,K., Duan, X., Joannopoulos,J. D.and Kimerling,L. C.,"Tunable multichannel optical filter based on silicon photonic band gap materials actuation," Appl. Phys. Lett. 81(22), 4112-4114 (2002).
[8] Pucker,G., Mezzetti,A., Crivellari,M., Bellutti,P. and Lui, A., Daldosso, N. and Pavesi, L., "Silicon-based near-infrared tunable filters filled with positive or negative dielectric anisotropic liquid crystals," Journal of Appl. Phys., 95(2), (2004).
[9] Niemi, T., Uusimaa, M., Tammela,S., Heimala,P., Kajava, T., Kaivola, M. and Ludvigsen, H., "Tunable Silicon Etalon for Simultaneous Spectral Filtering and Wavelength Monitoring of a DWDM Transmitter," IEEE PTL 13(1), 58 (2001).
[10] Tolmachev, V., Perova, T., Krutkova, E., Khokhlova, E., "Elaboration of the gap map method for the design and analysis of one-dimensional photonic crystal structures", Physica E: Low-dimensional Systems and Nanostructures, 41, 1122-1126 (2009).
[11] Yi, Zh. and Qi, W.,"Properties of photonic bandgap in one-dimensional multicomponent photonic crystal", Optoelectronics Lett., 2(1), 15 (2006).
[12] Glushko, A., Karachevtseva, L., "PBG properties of three-component 2D photonic crystals", Photon. Nanostruct., 4, 141-145 (2006).
[13] Rybin, M.V., Baryshev, A.V., Khanikaev, A.B., Inoue, M., Samusev, K.B., Sel'kin, A.V., Yushin, G. and Limonov, M.F., "Selective manipulation of stop-bands in multi-component photonic crystals: Opals as an example", Phys. Rev. B. 77, 205106 (2008).
[14] Tolmachev, V. A., Baldycheva, A. V., Dyakov, S. A., Berwick, K. and Perova T. S., "Optical Contrast Tuning in Three-Component One-Dimensional Photonic Crystals," J. of Lightwave Tech., 28(10), 1521-1529 (2010).
[15] Fink, Y., Winn, J.N., Shanhui, F., Chiping, C., Kimerling, L.C., "A dielectric omni-directional reflector", IEEE J. Sel. Top. Quantum Electron, 12, 1345 (2006).
[16] Chigrin, D.N., Lavrinenko, A.V., Yarotsky, D.A., Gaponenko, S.V., "Observation of total omnidirectional reflection from a one-dimensional dielectric lattice," Appl.Phys. A, 68, 25-28 (1999).
[17] Russell, P.St.J., Tredwell, S., Roberts, P.J., "Full photonic bandgaps and spontaneous emission control in 1D multilayer dielectric structures," Opt.Commun., 160, 66-71 (1999).
[18] Joannopoulos, J.D., Meade, R.D., Winn, R.D., [Photonic Crystals], Princeton University Press, P.184, (1995). Joannopoulos, J.D., Winn, S.G., Meade, R.D., [Photonic Crystals. Molding the Flow of Light], 2nd ed., Princeton University Press, (2008).
[19] Tolmachev, V. A., Astrova, E. V., Pilyugina, Yu. A., Perova, T. S., Moore, R. A. and Vij, J. K. "1D photonic crystal fabricated by wet etching of silicon", Optical Materials, 28(5) 831-835 (2005).
[20] Azzam, R. M. A., Bashara, N. M., [Ellipsometry and polarized light], Amsterdam, North-Holland, P.334 (1977).

[21] Tolmachev, V. A., Perova, T. S. and Berwick, K.,"Design criteria and optical characteristics of one-dimensional photonic crystals based on periodically grooved silicon," Appl. Opt., 42, 5679-5683 (2003).
[22] Tolmachev, V.A., Perova, T.S.and Moore, R.A., "Method of construction of composite one-dimensional photonic crystal with extended photonic band gaps," Opt. Express, 13(21), 8433-8441 (2005).
[23] Tolmachev, V. A., Astrova, E.V., Perova, T.S., Zharova, J.A, Grudinkin, S.A., Melnikov, V.A., "Electro-tunable in-plane one-dimensional photonic structure based on silicon and liquid crystal", App. Phys. Lett., 90**,** 011908 (2007).
[24] Tolmachev, V. A., Perova, T.S. and Berwick, K., "Design of 1D composite photonic crystals with an extended photonic band gap," J. Appl. Phys. 99, 033507 (2006).
[25] Tolmachev, V. A., Perova, T. S., Ruttle, J. and Khokhlova, E., "Design of One-dimensional Photonic Crystals Using Combination of Band Diagrams and Photonic Gap Map Approaches", J.Appl.Phys. 104, 033536 (2008).
[26] Tolmachev, V.A., Baldycheva, A.V., Krutkova, E.Yu., Perova, T.S. and Berwick, K., "Optical characteristics of a one-dimensional photonic crystal with an additional regular layer", Proc. of SPIE, 7390, 739017 (2009).
[27] Palik, E.D., [Handbook of Optical Constants of Solids], Academic Press (1998).
[28] Gurevich, E.L., Kittel, S., Hergenroder, R., Astrov, Yu. A., Portsel, L. M., Lodygin, A. N., Tolmachev, V. A. and Ankudinov, A. V., "Modification of GaAs surface by low-current Townsend discharge," J. Phys. D: Appl. Phys., 43, 275302 (2010).
[29] Tolmachev, V.A., Perova, T.S., Astrova, E.V., Volchek, B.Z. and Vij. J.K., "Vertically etched silicon as 1D photonic crystal," Phys. Stat. sol. (a), 197 N 2,544-548 (2003).